Jennifer Ziello, Derek Papalegis, Lily Vu, Kelsey Goldman, Jean Loebelenz, Shelby Sponaugle, Sasha Tkachev, Sarah Klein |
Cell Signaling Technology, Inc., Danvers MA 01923
Abstract #1156

A systematic comparison of common multiplex immunohistochemistry (mIHC) methodologies to the novel SignalStar™ assay in the characterization of the tumor microenvironment (TME).

INTRODUCTION

The emergence of an increasing number of immunotherapy biomarkers and their importance within the spatial context of the TME has resulted in a concomitant need for reliable and accurate multiplex immunohistochemical (mIHC) assays. Many of the currently available mIHC technologies do not offer amplification, resulting in the loss of detection of low expressing cells, while others require deposition and cycling of antibodies, which can lead to umbrella effects and epitope degradation, respectively. The SignalStar mIHC assay from Cell Signaling Technology is a novel methodology used to label, amplify and visualize up to 8 targets within the same formalin fixed, paraffin-embedded carcinoma (FFPE) tissue section without the need for fluorophore deposition or antibody cycling.

METHODS

In this study, the SignalStar mIHC assay was used to simultaneously label 8 targets including TIM-3, PD-1, PD-L1, LAG3, CD3, CD68, CD8 and Pan-Keratin in FFPE carcinoma tissue. A network of complementary, fluorescently-labeled oligonucleotides was used to amplify the signal of the first 4 antibody-oligo conjugates, followed by tissue imaging. The fluorescent signal was then removed, and the process repeated. The resulting two 4-plex images were then computationally aligned with QuPath. This methodology was compared to the Tyramide Signal Amplification (TSA) deposition assay, as well as to indirect and direct immunofluorescent (IF) detection with respect to mean fluorescence intensity (MFI) per cell and percent positivity of cells in matched regions of interest in serial sections. All mIHC strategies were in turn compared to the canonical chromogenic IHC assay. Furthermore, the fluorescent signal from the 8-plex SignalStar assay was removed and the same tissue was stained with fluorescent direct conjugates to achieve even higher plex.

RESULTS

SignalStar mIHC staining displayed strong, specific signal in all four channels and in both imaging rounds that matched that of the standard chromogenic IHC assay both visually and quantitatively. Furthermore, the SignalStar mIHC assay resulted in similar values of positive cells when compared to TSA and chromogenic detection. Despite achieving similar levels of positivity and signal intensity to that of TSA, the SignalStar assay required less optimization, and did not suffer from steric hindrance associated with tyramide deposition (also known as the umbrella effect). Depending on the relative abundance of target expression, indirect IF detection often resulted in comparable percent positivity to that produced by SignalStar and TSA, while direct IF detected lower percent positive cells than all other techniques. In addition, direct IF detection in the 488 and 594 channels was not possible due to the low signal intensity unable to overcome the level of autofluorescence present in the tissue. Direct IF displayed comparable percent positivity to that achieved by chromogenic IHC only when detecting abundant targets, such as CD8. Importantly, these more abundant targets were successfully stained using direct IF following completion of the 8-plex SignalStar assay, demonstrating the ability to achieve a higher plex by combining these two assays.

CONCLUSIONS

Our data demonstrates that SignalStar mIHC detected similar percentages of cells when compared to chromogenic and TSA staining. Alternatively, SignalStar mIHC outperformed direct and indirect immunofluorescence detection of less abundant targets, indicating that signal amplification may be required for accurate detection of these targets. Importantly, SignalStar mIHC overcomes some of the challenges involved with the TSA assay. When compared to TSA, SignalStar mIHC requires less optimization to achieve a higher plex, and enables detection of multiple biomarkers within the same subcellular compartment of the same cell. The SignalStar protocol was also successfully combined with a panel of direct conjugates, showing the complementarity of these assays in such a way that both plex and flexibility can be increased. Ultimately, we demonstrate that SignalStar mIHC is a useful tool in the characterization and analysis of the complex TME.

Figure 1: How SignalStar mIHC Works

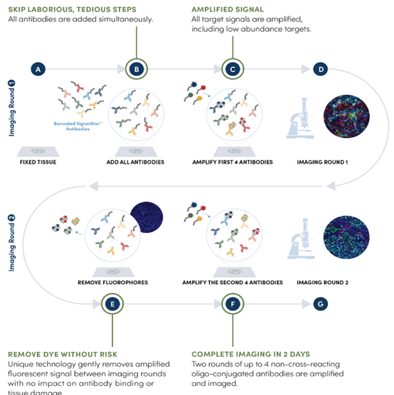

The SignalStar assay allows for the simultaneous labeling of up to 8 targets in formalin-fixed paraffin embedded (FFPE) tissue. Deparaffinized and rehydrated FFPE tissue sections undergo antigen retrieval (A), and all antibodies in your plex-size of choice (3-8 maximum unique oligo-conjugated antibodies) are added in one primary incubation step (B). A network of complementary oligos with fluorescent dyes (excitations: 488, 594, 647, 750) amplify the signal of up to 4 antibodies in the first round of imaging (C-D). If the plex-size is greater than 4, the first round of oligonucleotides and fluorophores are gently and specifically removed (E), and a second round of amplification is performed to visualize up to 4 additional oligo-conjugated antibodies (F). The two images are then aligned and fused computationally with either proprietary or open-source software to generate the full up to 8-plex image (G).

Figure 2: 8-plex SignalStar mIHC Matches Chromogenic

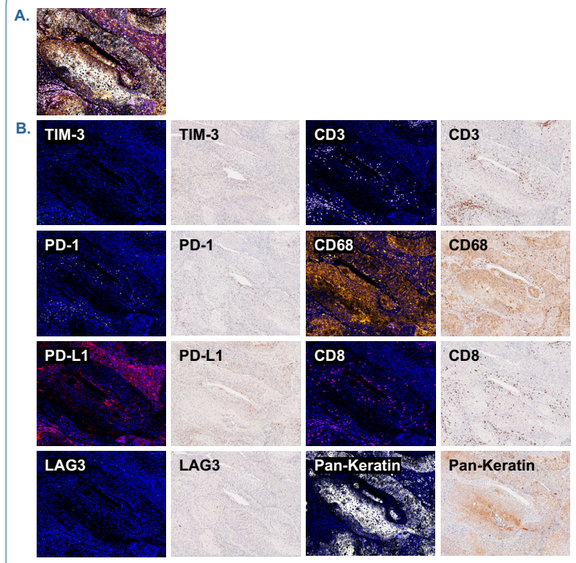

A) SignalStar multiplex immunohistochemical staining of paraffin-embedded human head and neck carcinoma using TIM-3 (D5D5R™) & CO-00010-488 SignalStar™ Oligo-Antibody Pair #81365 (green), PD-1 (Intracellular Domain) (D4W2J) & CO-0008-594 SignalStar™ Oligo-Antibody Pair #35347 (yellow), PD-L1 (E1L3N®) & CO-0005-647 SignalStar™ Oligo-Antibody Pair #52085 (red), LAG3 (D2G4O™) & CO-0026-647 SignalStar™ Oligo-Antibody Pair #40966 (cyan), CD3ε (D7A6E™) & CO-0001-488 SignalStar™ Oligo-Antibody Pair #92856 (pink), CD68 (D4B9C) & CO-0007-594 SignalStar™ Oligo-Antibody Pair #77318 (orange), CD8α (D8A8Y) & CO-0004-647 SignalStar™ Oligo-Antibody Pair #66676 (magenta), and Pan-Keratin (C11) & CO-0003-750 SignalStar™ Oligo-Antibody Pair #97227 (white). B) SignalStar immunohistochemical staining of paraffin-embedded human head and neck carcinoma using the SignalStar antibodies described above compared to chromogenic staining of serial sections using TIM-3 (D5D5R) XP® rabbit mAb #45208, PD-1 (Intracellular Domain) (D4W2J) XP® Rabbit mAb #86163, PD-L1 (E1L3N®) XP® Rabbit mAb #13684, LAG3 (D2G4O) XP® Rabbit mAb #15372, CD3ε (D7A6E™) XP® Rabbit mAb #85061, CD68 (D4B9C) XP® Rabbit mAb #76437, CD8α (D8A8Y) Rabbit mAb #85336 and Pan-Keratin (C11) Mouse mAb #4545.

Figure 3: SignalStar Shows a Similar Percentage of Positive Cells When Compared to Other Amplification Methodologies

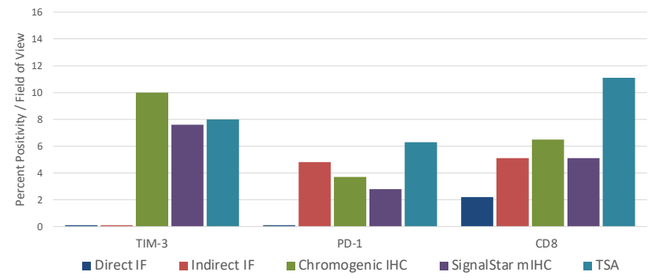

A quantitative comparison of the percent positive cells per field of view of various targets as achieved by staining with direct IF, indirect IF, chromogenic immunohistochemistry (IHC), SignalStar mIHC, and TSA in paraffin-embedded human head and neck carcinoma. Positive cells in matching regions of interest (ROIs) from semi-serial sections were quantified with the inForm Tissue Analysis software from Akoya. Thresholds were defined visually. Direct staining was performed using TIM-3 (D5D5R™) XP® Rabbit mAb (Alexa Fluor® 488 Conjugate) #54669, (PD-1 (Intracellular Domain) (D4W2J) XP® Rabbit mAb (Alexa Fluor® 594 Conjugate), and CD8α (D8A8Y) Rabbit mAb (Alexa Fluor® 647 Conjugate) #28512 **(blue bars)**. Indirect staining with secondary antibodies was performed with TIM-3 (D5D5R™) Rabbit mAb #45208 followed by detection with Anti-rabbit IgG (H+L), $F(ab')_2$ Fragment (Alexa Fluor® 488 Conjugate) #4412, PD-1 (Intracellular Domain) (D4W2J) XP® Rabbit mAb #86163 followed by detection with Anti-rabbit IgG (H+L), $F(ab')_2$ Fragment (Alexa Fluor® 594 Conjugate) #8889, and CD8α (D8A8Y) Rabbit mAb #85336 followed by detection with Anti-rabbit IgG (H+L), $F(ab')_2$ Fragment (Alexa Fluor® 647 Conjugate) #4414 **(red bars)**. Chromogenic staining was performed using TIM-3 (D5D5R™) Rabbit mAb #45208, PD-1 (Intracellular Domain) (D4W2J) XP® Rabbit mAb #86163, and CD8α (D8A8Y) Rabbit mAb #85336 **(green bars)**. SignalStar staining was performed using TIM-3, PD-1, and CD8α SignalStar Oligo-Antibody Pairs from Figure 2 **(purple bars)**. TSA detection was performed using TIM-3 (D5D5R™) Rabbit mAb #45208, PD-1 (Intracellular Domain) (D4W2J) XP® Rabbit mAb #86163, and CD8α (D8A8Y) Rabbit mAb #85336, followed by detection with Opal Detection reagents from Akoya (NEL811001KT) **(teal bars)**.

Figure 4: SignalStar Overcomes the Umbrella Effect

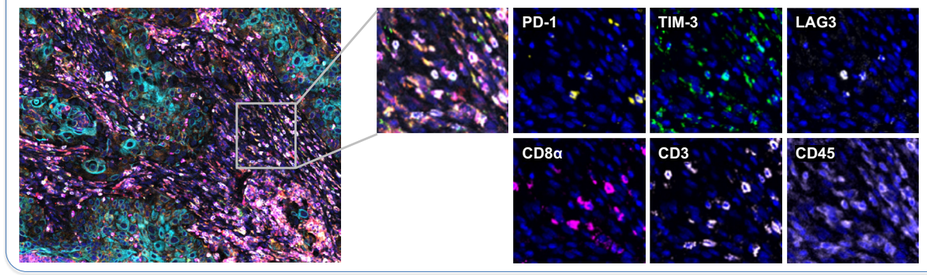

SignalStar immunofluorescent signal from PD-1, TIM-3, LAG3, CD8α, CD3, and CD45 co-localizes to the same subcellular compartment (cell membrane) of the same cell. SignalStar is able to overcome the umbrella effect from epitope masking that is commonly observed with other multiplex assays. Paraffin-embedded human and neck carcinoma tissue was stained as described in Figure 2.

Figure 5: SignalStar Can be Combined with Direct Immunofluorescence to Achieve a Higher Plex

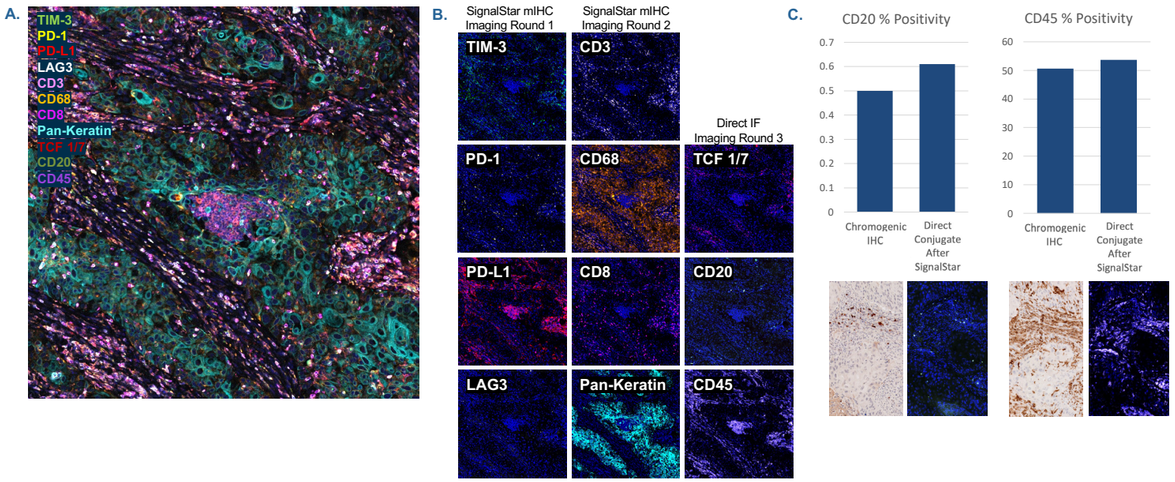

A) and B) Multiplex immunohistochemical staining of paraffin-embedded human head and neck carcinoma using the 8-plex SignalStar panel described in Figure 1B, followed by staining with TCF1/TCF7 (C63D9) Rabbit mAb (Alexa Fluor® 594 Conjugate) #35972 (burgundy), CD20 (E7B7T) XP® Rabbit mAb (Alexa Fluor® 647 Conjugate) #83399 (olive), and CD45 (Intracellular Domain) (D9M8I) XP® Rabbit mAb (Alexa Fluor® 750 Conjugate) #16529 (purple). C) Quantitative comparison of the % positivity of CD20 and CD45 signal as achieved by staining with CD45 (Intracellular Domain) (D9M8I) XP® Rabbit mAb #13917 followed by detection with SignalStain® Boost IHC Detection Reagent (HRP, Rabbit) #8114 and SignalStain® DAB Substrate Kit #8059 (left) and CD20 (E7B7T) XP® Rabbit mAb (Alexa Fluor® 647 Conjugate) #83399 following SignalStar staining (right). C). Corresponding images of direct conjugate and chromogenic staining that were quantified in the graph above.

Jennifer Ziello
email: Jennifer.Ziello@cellsignal.com
cellsignal.com/posters